Molecular Vision 2019; 25:821-833 <http://www.molvis.org/molvis/v25/821>
Received 13 August 2019 | Accepted 30 November 2019 | Published 2 December 2019

Spectrum, frequency, and genotype–phenotype of mutations in *SPATA7*

Xueshan Xiao, Wenmin Sun, Shiqiang Li, Xiaoyun Jia, Qingjiong Zhang

(The first three authors contributed equally to this work.)

State Key Laboratory of Ophthalmology, Zhongshan Ophthalmic Center, Sun Yat-sen University, 54 Xianlie Road, Guangzhou, China

Purpose: To describe the mutation spectrum of *SPATA7* and associated ocular phenotypes.
Methods: As part of a continuing examination of the genetic basis of inherited ophthalmic diseases, sequencing variations in *SPATA7* were identified in sequencing data from 5,090 probands. Mutations in *SPATA7* were identified in 12 Chinese patients from ten families. Family history and clinical data were examined in detail in these patients. To evaluate possible gene-specific fundus changes, the results were combined with data from 66 patients from 50 families previously reported in the literature.
Results: Seven homozygous or compound heterozygous mutations, including two novel mutations (c.367C>T, p.Q123* and c.1083–2A>G) and five known mutations in *SPATA7*, were identified in ten families, including six families with Leber congenital amaurosis (LCA), three families with juvenile retinitis pigmentosa, and one family with early-onset high myopia. These families accounted for approximately 2.2% (6/269) of LCA and 0.4% (10/2,252) of inherited retinal dystrophies in this case series. A combined analysis of data from the present study and data from 60 families reported in the literature showed that 93.3% (112/120) of mutant alleles were truncation mutations, whereas only about 5.0% were missense mutations, and 1.7% were non-frameshift indels. Common *SPATA7*-associated fundus changes, including narrow arterioles, a relatively well-preserved macular region, and widespread RPE atrophy resulting in diffuse mottled hypopigmentation in the midperipheral retina, were identified in this cohort and in patients in the literature. Missense mutations were not associated with specific phenotypic features or severity.
Conclusions: Narrow arterioles, a relatively well-preserved macular region, and widespread RPE atrophy resulting in diffuse mottling hypopigmentation in the midperipheral retina may be considered early and common fundus changes specific to *SPATA7*-associated retinopathy. The fact that similar mutations result in varied phenotypes points to the existence of other potential modifiers of the disease. Uncovering the identity of these modifiers might aid the development of novel treatments.

Hereditary retinal degeneration (HRD) includes a broad group of hereditary retinal disorders with different patterns of inheritance, varied clinical phenotypes, and a highly polymorphic basis of molecular defects. These disorders are further classified into several subgroups based on the primary involvement of cones or rods, location of the retina, severity of the disease, and accompanying ocular or systemic signs. The disorders can be transmitted as autosomal dominant, autosomal recessive, X-linked, or mitochondrial traits. Thus far, mutations in at least 271 genes have been reported to be responsible for these disorders (RetNet, https://sph.uth.edu/retnet/). A systematic analysis of the coding regions of these genes identified genetic defects in approximately 50–60% of families with HRDs. A lack of mutations in these genes may suggest a genetic defect either in undefined novel genes or in uncovered regions of known genes. However, a proportion of reported mutations may not truly be causative of disease. Clarification of genotype–phenotype correlations, especially gene-specific retinal lesions, will not only help to further identify genetic defects but also clarify the pathogenesis of mutations.

Mutations in the *spermatogenesis-associated protein 7* (*SPATA7*) gene (Gene ID: 55812, OMIM: 609868) have been reported to be responsible for autosomal recessive Leber congenital amaurosis (LCA), retinitis pigmentosa (RP), juvenile RP, and cone or cone-rod dystrophy (CORD) [1-33]. To date, biallelic mutations in *SPATA7* have been reported in 54 families. However, the spectrum and frequency of mutations in *SPATA7* and their associated characteristic phenotypes have not been systemically analyzed.

In the present study, we systematically analyzed variations in *SPATA7*, mainly based on a combination of whole exome and targeted exome in-house sequencing data from

Correspondence to: Qingjiong Zhang, State Key Laboratory of Ophthalmology, Zhongshan Ophthalmic Center, Sun Yat-sen University, 54 Xianlie Road, Guangzhou 510060, China; Phone: (+86)-20-66677083; FAX: (+86)-20-66686996; email: zhangqji@mail.sysu.edu.cn; zhangqingjiong@gzzoc.com

5,090 unrelated patients. Seven biallelic mutations in *SPATA7*, including two novel mutations, c.367C>T (p.Q123*) and c.1083–2A>G, were observed in ten families, including four families briefly reported previously. Systemic analysis of these genotype–phenotype data, as well as related data in the literature, shed light on the spectrum and frequency of mutations in *SPATA7* and identified gene-specific changes in the early developmental stage, in addition to novel fundus changes.

METHODS

Venous blood was collected in an EDTA coating tube from superficial vein of the arm of each participant using disposable needle after sterilization of skin. The blood samples were stored at 4 °C temporarily for a few hours to a few days before the preparation of genomic DNA. Clinical data were collected from outpatient clinics following the Guidance of Sample Collection of Human Genetic Diseases (863-Plan) by the Ministry of Public Health of China. Written informed consent adherent to the tenets of the Declaration of Helsinki as well as the ARVO statement on human subjects was obtained from all the patients or their guardians before sample and data collection. This study was approved by the institutional review board of the Zhongshan Ophthalmic Center.

Genomic DNA was prepared from leukocytes obtained from the venous blood of the study group. Genetic defects in the probands of each family were screened with either whole exome sequencing (WES) or targeted exome sequencing (TES), and a mutation in one individual was identified with Sanger sequencing (Table 1). The WES or TES data were analyzed through multistep bioinformatics analysis as described previously [34,35]. Variants in *SPATA7* were obtained for 5,090 probands with a variety of forms of genetic eye diseases, including 2,252 probands with HRDs (one proband was examined with Sanger sequencing, 2,132 probands were examined with WES described previously, and 119 additional probands were recently examined with TES).

Homozygous or compound heterozygous rare variants in *SPATA7* were selected for this study, and their segregation in family members was confirmed with Sanger sequencing. The clinical data and mutation characteristics in the patients were systematically analyzed in conjunction with data reported in the literature [1-33]. The ophthalmic examinations, including visual acuity, axial length, refraction, fundus changes, and electroretinogram, were performed as we described in previous studies [36]. Gene-specific fundus changes were determined by comparing available fundus images with detailed documented descriptions and available clinical data from these patients, as well as from case studies reported in the literature. Factors affecting phenotypic changes were considered, including the type and location of mutations and the patient's age at the time of the examination.

RESULTS

Mutations in SPATA7 and phenotypes in the cohort: Based on an analysis of sequencing data collected at our clinic on 5,090 probands with genetic eye diseases (including 269 probands with LCA and 1,983 probands with other forms of HRDs), biallelic mutations in *SPATA7* were found in ten families, with 12 affected individuals (Figure 1, Table 1). The clinical diagnosis of the probands was LCA in six families, juvenile RP (or early-onset HRD) in three families, and early-onset high myopia in one family (Table 1). In total, seven different mutations were identified in these ten families. Of these mutations, five were known mutations, and two were novel mutations, of which the c.367C>T (p.Q123*) nonsense mutation was predicted to have a 35 score by CADD (https://cadd.gs.washington.edu/), and the c.1083–2A>G mutation was predicted to affect the splicing acceptor site by BDGP and HSF (Table 2). All mutations were confirmed with Sanger sequencing and segregated with disease in the families (Figure 1 and Appendix 1). Therefore, the mutations in *SPATA7* were responsible for 2.2% (6/269) of families with LCA and 0.4% (10/2,252, 269+1983) of families with HRD in this Chinese cohort from one institution. All seven mutations were predicted to result in truncated proteins when expressed.

Clinical data on the 12 patients in the ten families are summarized in Table 1, including nine male patients and three female patients. The age of onset varied from 3 months after birth to 22 years. Poor vision or no pursuit of objects was the most common initial sign and was present in nine of ten probands, while night blindness was the initial sign in the other patients. Visual acuity ranged from no pursuit of light to 0.6. Nonrecordable cone and rod responses were recorded in seven probands using electroretinography. Fundus changes were age-dependent, with some common features possibly specific to mutations in *SPATA7*.

Fundus images were available for six patients from five families, including one patient with fundus images taken at three different times. The youngest patient (F01-II:1) was a 9-month-old boy with no pursuit of light for 6 months. Electroretinography recordings in this case showed no recordable responses of rods and cones. A fundus examination revealed attenuation of retinal arterioles and a relatively normal-looking posterior retina, except the absence of foveal reflex. Tiny spot-like RPE atrophy formed a frosted appearance in the midperipheral retina (Figure 2A,B). A peculiar, novel fundus change was observed in two affected siblings

Table 1. Clinical information of the probands and affected siblings with biallelic SPATA7 mutations.

Family ID	Clinic group	Mutation based on NM_018418	Effect	Gender	Age (year) at		Axial length/ refraction	First symptom	Visual acuity		Fundus changes	ERG recording rods and cones
					onset	1st exam			right	left		
F01-II:1*	LCA	c.[1183C>T];[1183C>T]	p.[R395*];[R395*]	M	0.3	0.6	NA	PV, ODS, RN	NPL	NPL	AV, YFD	Extinguished
F02-II:1	LCA	c.[367C>T];[1183C>T]	p.[Q123*];[R395*]	F	FMB	4.3	+5.25; +5.75	PV, RV	LP	LP	AV, TD	NA
F03-II:1*	LCA	c.[644_647del];[644_647del]	p.[L215Sfs*];[L215Sfs*]	F	FMB	2.3	NA	PV, ODS, RN	LP	LP	AV, YSB	Extinguished
F03-II:2	LCA	c.[644_647del];[644_647del]	p.[L215Sfs*];[L215Sfs*]	M	FMB	1.3	NA	PV, ODS, RN	LP	LP	AV, YSB	NA
F04-II:1*	LCA	c.[1183C>T];[1183C>T]	p.[R395*];[R395*]	M	0.583333	1.3	NA	PV, ODS, RN	NPL	NPL	AV, TD	Extinguished
F05-II:1	LCA	c.[367C>T];[367C>T]	p.[Q123*];[Q123*]	F	FMB	13	NA	PV, RN	LP	LP	AV, YMD, PPP	Extinguished
F06-II:1	LCA	c.[322C>T];[322C>T]	p.[R108*];[R108*]	M	0.3	2.4	+5.00; +4.75	PV, RV	LP	LP	normal-like	Extinguished
F07-II:1*	jRP	c.[322C>T];[1183C>T]	p.[R108*];[R395*]	M	FMB	3.4	-1.50; -1.25	PV, NB, PA	0.4	0.6	AV, YMD, PPP	Extinguished
F08-II:1	jRP	c.[20_23del];[1183C>T]	p.[V7Efs*19];[R395*]	M	4	7	+3.00;+2.50	PV, NYS	0.02	0.03	AV, YMD, PPP	Extinguished
F09-II:6	jRP	c.[20_23del];[1083-2A>G]	p.[V7Efs*19];[splicing]	M	22	25	NA	NB	HM	LP	WPD, AV, IBP	NA
F10-II:1	myopia	c.[20_23del];[20_23del]	p.[V7Efs*19];[V7Efs*19]	M	NA	5	-8.50; -10.25	PV	NA	NA	NA	NA
F10-II:2	myopia	c.[20_23del];[20_23del]	p.[V7Efs*19];[V7Efs*19]	M	NA	3	24.38; 23.91mm	PV	NA	NA	NA	NA

M=male; F=female; FMB=first few months after birth; NA=not available; PV=poor vision or no pursuit of objects; ODS=ocular digital sign; RN=roving nystagmus; NB=night lindness; LP=light perception; NPL=No pursuit of light; HM=hand motion; AV=attenuated vessels; TD=tapetoretinal degeneration; YFD=Yellowish-white frosted degeneration in midperipheral retina; YSB=Yellowish-white sandy beach in midperipheral retina; YMD=Yellowish-white mottled degeneration in midperipheral retina. PPP=a few tiny pepper-powder like pigmentation; WPD=waxy pale disc; IBP=Irregular black pigmentation; NA=Not available; Ext=Extinguished.

when they were aged 2 years and 4 months (F03-II:1) and 1 year and 4 months (F03-II:2), with yellowish-white sand-like deposits in the midperipheral retina (Figure 2C–F). Interestingly, similar retinal degeneration was absent in part of the inferior portion, close to the area of the optic fissure in the left and right eyes of the two siblings. The posterior fundus and optic disc were relatively normal, except slightly attenuated retinal arterioles (Figure 2C–F). In addition, diffuse and mottling hypopigmentation in the midperipheral retina was observed in probands from two families (F05-II:1, Figure 2G,H; F07-II:1, Figure 2I).

Age-related fundus changes were observed in the proband from F07. Fundus images for F07-II:1 were obtained when the patient was aged 3 years and 5 months (Figure 3 A), 7 years and 5 months (Figure 3B,C), and 8 years and 7 months (Figure 3D–I). The proband attended our clinic at the ages of 3 years and 5 months due to a complaint of "bumping into obstacles." Ocular examination revealed a relatively normal

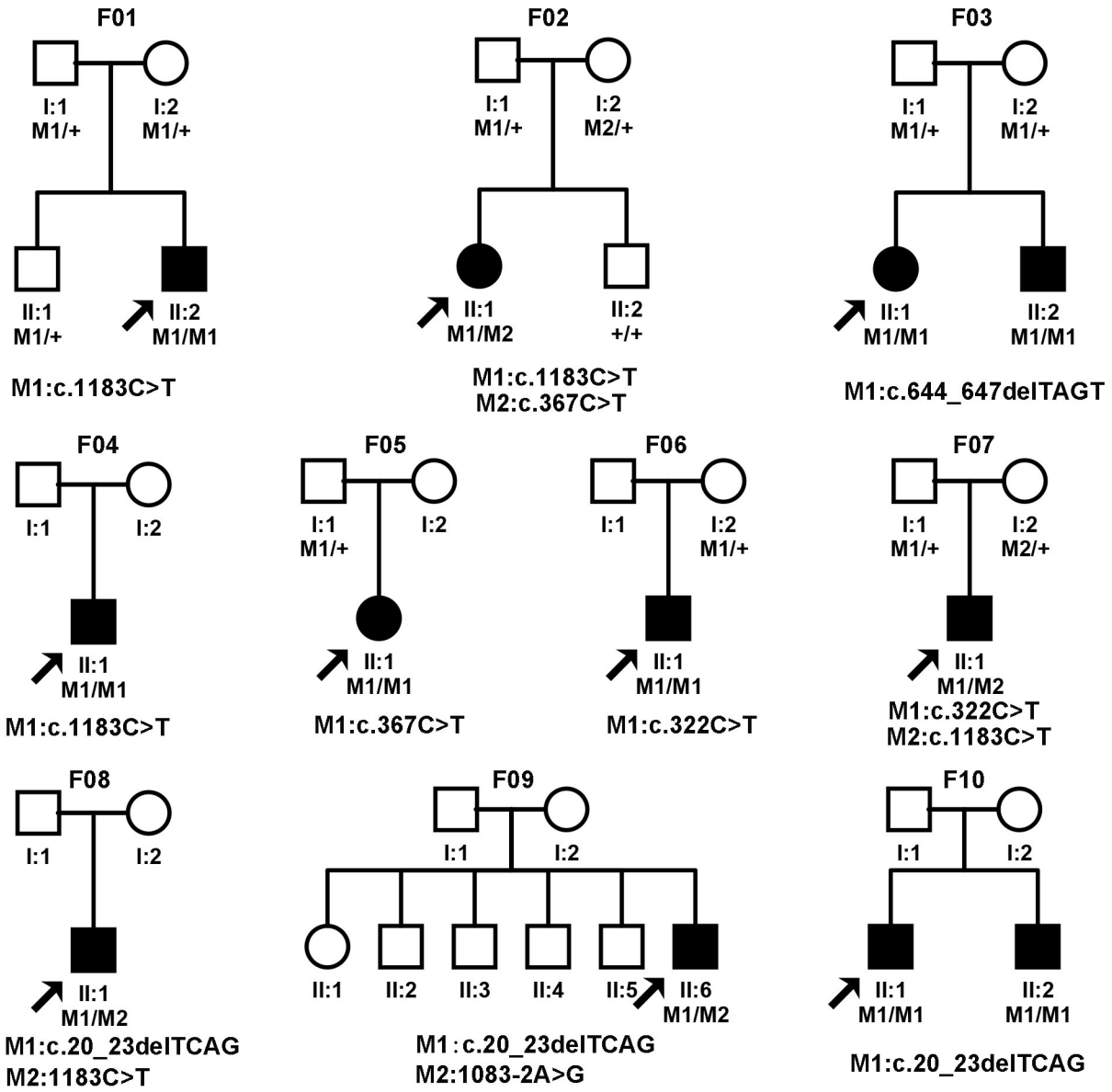

Figure 1. Pedigrees of ten families with biallelic mutations in *SPATA7*. The arrow indicates the proband in each family. The affected individuals are shown as filled squares (male) or circles (female). Mutations are listed under each family, and their segregation in families is shown in the pedigrees.

Table 2. Mutations in SPATA7 identified in this study and previous literatures.

Position at chr14	Nuleotide change NM_018418	Alleles in probands	Effect	Type	CADD score	REVEL score	BDGP	HSF	Frequency in ExAC	HGMD	Our cohort	First reported
88828457	c.1-23706_372+8679delinsTGG	2	/	Gross deletion	/	/	/		/	DM	/	[12]
88852165	c.3G>A	1	p.?	Initiation	24.7	0.277	/	/	1/79940	DM	/	[6]
88852180	c.18A>G	2	p. =	Splicing	/	/	LDS	BDS	/	DM	/	[27]
88852181	c.19G>A	2	p.V7I	Missense +Splicing	/	/	LDS	BDS	/	DM	/	[23]
88857725	c.20_23delTCAG	5	p.V7Efs*19	Frameshift	/	/	/	/	/	DM	Yes	[32]
88859831	c.189delA	1	p.A64Lfs*3	Frameshift	/	/	/	/	/	DM	/	[31]
88883061	c.245dupA	1	p.D82Efs*16	Frameshift	/	/	/	/	/	DM	/	[31]
88883069	c.253C>T	13	p.R85*	Nonsense	37	/	/	/	2/120686	DM	/	[3]
88883081	c.265_268delCTCA	1	p.L89Kfs*4	Frameshift	/	/	/	/	/	DM	/	[3]
88883104	c.288T>A	12	p.C96*	Nonsense	29	/	/	/	2/120690	DM	/	[15]
88883112	c.296_297delAG	2	p.E99Vfs*5	Frameshift	/	/	/	/	/	DM	/	[22]
88883138	c.322C>T	11	p.R108*	Nonsense	35	/	/	/	4/119988	DM	Yes	[1]
88883156	c.341delA[†1]	1	p.N114Ifs*23	Frameshift	/	/	/	/	/	DM	/	[13]
88883183	c.367C>T	3	p.Q123*	Nonsense	35	/	/	/	/	/	Yes	Novel
88892575	c.373-1G>A[†2]	1	/	Splicing	/	/	LAS	BAS	/	DM	/	[13]
88892690	c.487A>T	1	p.K163*	Nonsense	35	/	/	/	/	DM	/	[11]
88892843	c.640delC[†3]	2	p.Q214Sfs*2	Frameshift	/	/	/	/	/	DM	/	[7]
88892847	c.644_647delTAGT	2	p.L215Sfs*30	Frameshift	/	/	/	/	/	/	Yes	[20]
88892903	c.700dupT	1	p.S234Ffs*2	Frameshift	/	/	/	/	/	DM	/	[29]
88892911	c.708_711delACAA	1	p.K236Nfs*9	Frameshift	/	/	/	/	/	DM	/	[29]
88892966	c.763C>T	3	p.Q255*	Nonsense	39	/	/	/	/	DM	/	[2]
88893049	c.845+1G>A	3	/	Splicing	/	/	LDS	BDS	1/112364	DM	/	[2]
88895690	c.913-2A>G	4	/	Splicing	/	/	LAS	BAS	/	DM	/	[14]
88895739	c.960dupA[†4]	4	p.P321Tfs*6	Frameshift	/	/	/	/	/	DM	/	[1]
88897545	c.1058dupC	1	p.S354Ffs*4	Frameshift	/	/	/	/	/	DM	/	[19]
88899477	c.1083-2A>G	1	/	Splicing	/	/	LAS	BAS	/	/	Yes	Novel
88899496	c.1100A>G	1	p.Y367C	Missense	26.9	0.522	/	/	2/120094	DM	/	[30]
88899498	c.1102_1103delCT	2	p.L368Efs*4	Frameshift	/	/	/	/	/	DM	/	[11]
88899508	c.1112T>C	2	p.I371T	Missense	25.5	0.234	/	/	39/120050	DM?	Yes	[24]
88903886	c.1161-1G>C	1	/	Splicing	/	/	LAS	BAS	1/120856	DM	/	[2]
88903897	c.1171C>T	3	p.R391*	Nonsense	44	/	/	/	/	DM	/	[23]

Position at chr14	Nuleotide change NM_018418	Alleles in probands	Effect	Type	CADD score	REVEL score	BDGP	HSF	Frequency in ExAC	HGMD	Our cohort	First reported
88903909	c.1183C>T	13	p.R395*	Nonsense	36	/	/	/	4/120876	DM	Yes	[1]
88903937	c.1211A>G	1	p.E404G	Missense	29.8	0.157	/	/	/	DM	/	[26]
88903941	c.1215G>T	2	p.E405D	Missense	24.4	0.113	/	/	1/120540	DM	/	[13]
88903946	c.1215+5G>A	2	/	Splicing	/	/	none	BDS	/	DM	/	[27]
88904180	c.1216-2A>T	2	/	Splicing	/	/	LAS	BAS	/	DM	/	[13]
88904181	c.1216-1G>A	2	/	Splicing	/	/	LAS	BAS	/	DM	/	[8]
88904195	c.1229_1231delACC[†5]	1	p.H410del	Inframe deletion	/	/	/	/	/	DM	/	[3]
88904207	c.1241_1252del12	1	p.V414_V417del	Inframe deletion	/	/	/	/	/	DM?	/	[19]
88904339	c.1373delT	4	p.V458Efs*48	Frameshift	/	/	/	/	/	DM	/	[8]
88904361	c.1395delA[†6]	2	p.Q465Hfs*41	Frameshift	/	/	/	/	/	DM	/	[1]

Notes: LDS, loss of a donor site; LAS, loss of an acceptor site; BDS, Broken Donor Site; BAS, Broken Acceptor Site. †1, previously reported as c.340del; †2, previously reported as c.371-1G>A; †3, previously reported as c.544delC based on NM_018418; †4, some previously reported as c.961dupA; †5, previously named as c.1227_1229delCAC; †6, previously named as c.1546delC. None of the 41 mutations was present in 1000 genome.

Molecular Vision 2019; 25:821-833 <http://www.molvis.org/molvis/v25/821>

posterior retina (Figure 3A), with a few minor grayish-white spots in the midperiphery. Electroretinography demonstrated nonrecordable responses for rods and cones. By the time the child was 7 years and 5 months, the grayish-white spots on the midperipheral retina were clearly obvious (Figure 3B,C). At the age of 8 years and 7 months, diffuse and mottling hypopigmentation with a few small intraretinal pigments of midperipheral retina was visible, displaying a salt-and-pepper appearance in the focal area (Figure 3D–I). In addition, a salt-and-pepper-like fundus change was recorded in F08-II:1 when the child was 7 years old. Bone spicule-like pigmentation in the midperiphery was recorded in one patient (F09-II:6) at the age of 25 years, indicating that fundus changes may worsen with age. Based on a comparison of the fundus images with documented descriptions of fundus changes in the case records, in some patients, a fundus with a relatively normal-looking posterior retina (macular region) would likely be described as normal by some ophthalmologists in general outpatient clinics, despite the presence of significant degeneration in the midperiphery. In summary, the age-related change in the fundus observed in patient F07-II:1 with time may be common in patients with mutations in *SPATA7*, as discussed in the phenotypic characterization section.

DISCUSSION

In this study, the clinical phenotypes of 12 patients from ten families with biallelic mutations in *SPATA7* were described, including six families with newly identified c.367C>T (p.Q123*) and c.1083–2A>G mutations. Common age-dependent *SPATA7*-associated fundus changes were identified based on an analysis of these patients. The data suggested that

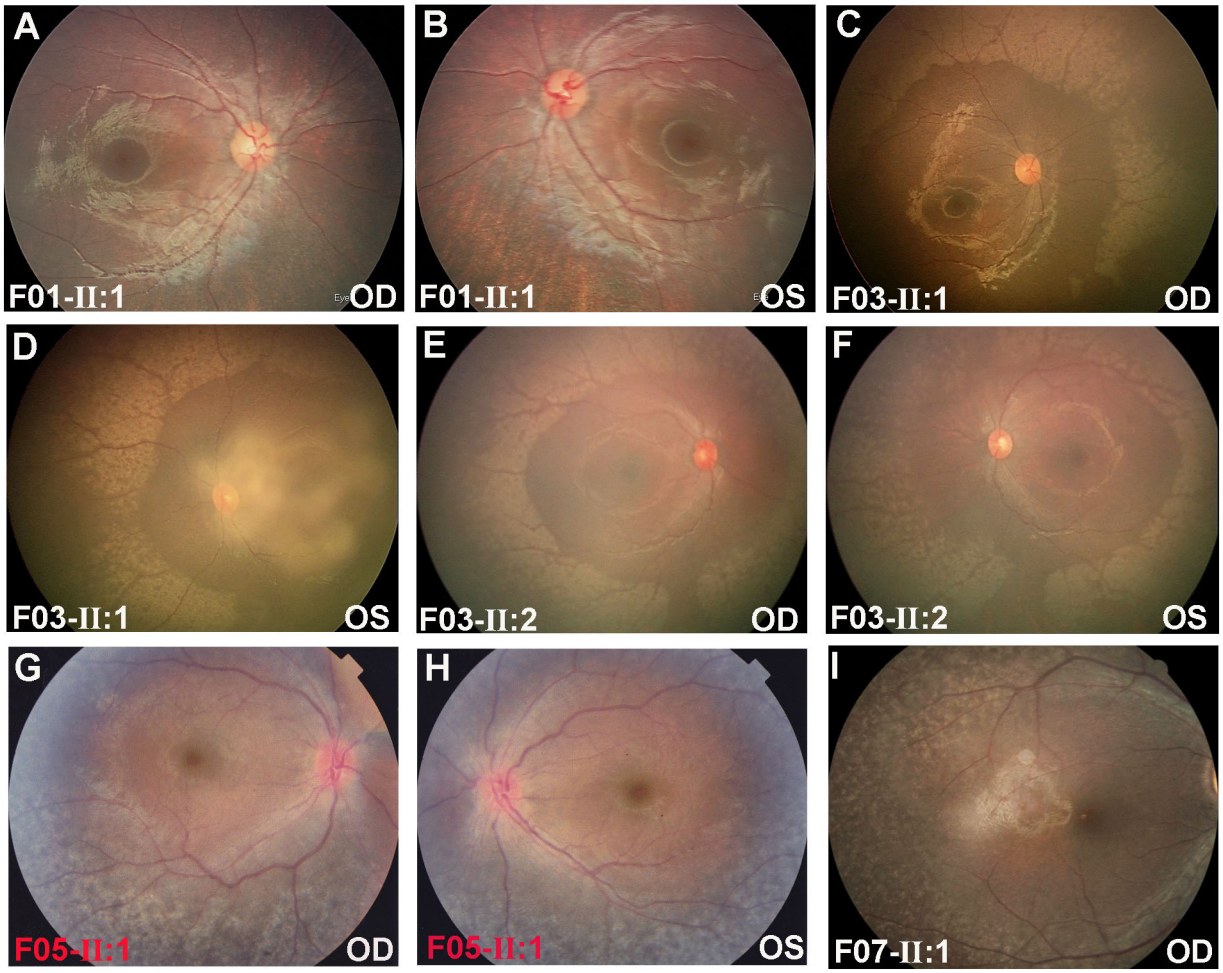

Figure 2. Fundus images from patients with biallelic mutations in *SPATA7*. Representative fundus images show yellowish-white frosted degeneration in the midperiphery in patient F01-II:1 (**A** and **B**) and yellowish-white sand-like deposits in the midperiphery sparing the inferior area close to the optic fissure (**C**–**F**), in addition to yellowish-white mottled degeneration in the midperiphery (**G**–**I**). The homozygous novel mutation c.367C>T was identified in the F05-II:1, which is highlighted in red in **G** and **H**.

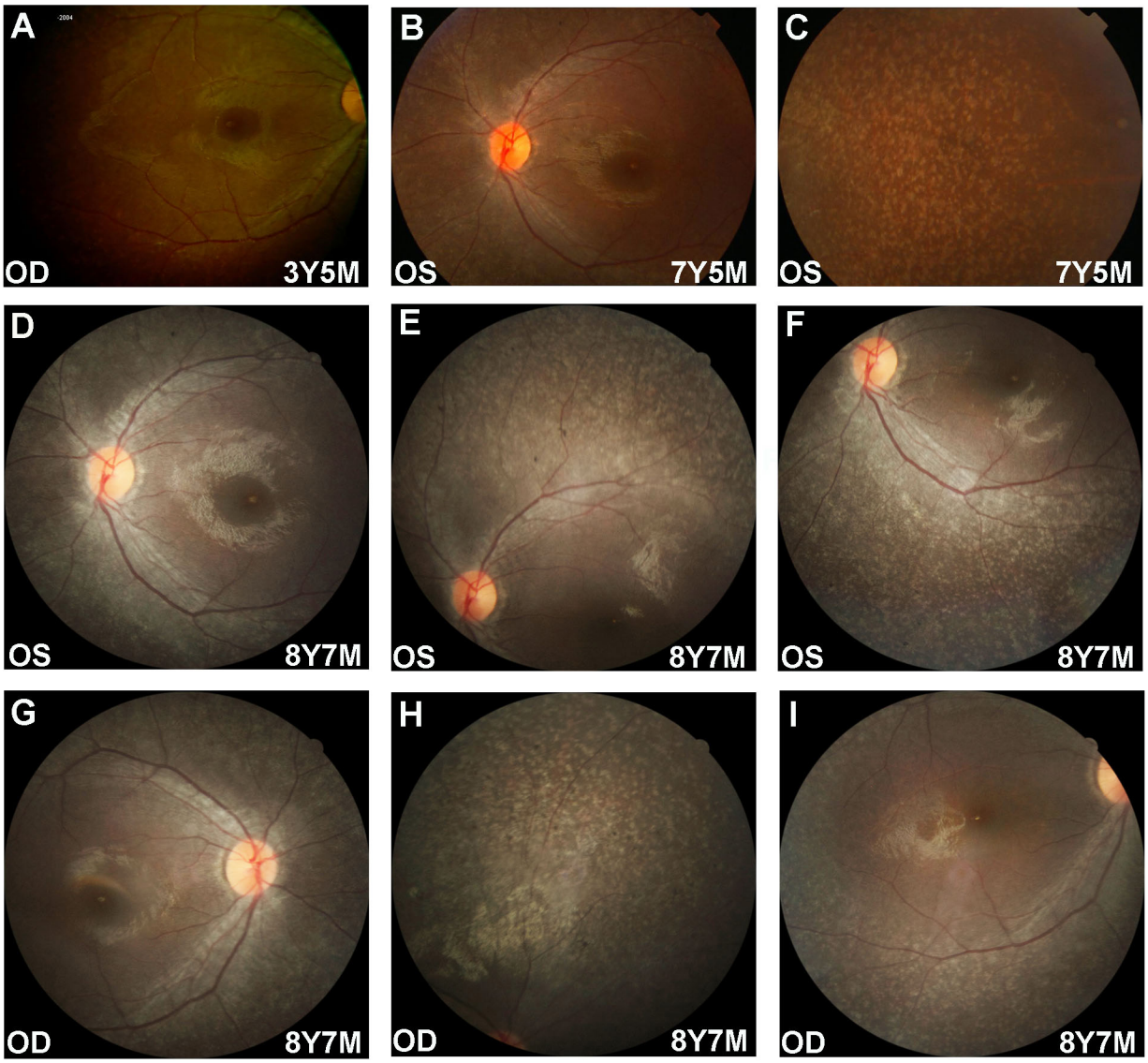

Figure 3. Fundus images showing age-dependent changes in a patient (F07-II:1). The fundus appeared nearly normal in the posterior area, with a few minor grayish-white spots in the midperiphery at the age of 3 years and 5 months (**A**), and progressed to significant yellowish-white spots in the midperiphery at the age of 7 years and 5 months (**B**, **C**). By the age of 8 years and 7 months, diffuse mottling hypopigmentation, with a few small intraretinal pigments, was visible (**D**–**I**). Mild salt-and-pepper-like changes were observed (**E**, **H**).

mutations in *SPATA7* may contribute to approximately 2.2% of LCA and 0.4% of HRD cases in Southern Chinese.

Biallelic mutations in *SPATA7* have been detected in a total of 78 patients in 60 families including those in this study and described in previous reports [1-33] involving 41 mutations (Table 2 and Appendix 2) based on transcript NM_018418.5. Fifty of the 60 families were described by other groups, and the other ten were from this study cohort. There are no reports of an association of heterozygous mutations in *SPATA7* with eye-related diseases. The 41 mutations could be classified as follows: nonsense (eight mutations in 59 alleles), frameshift (15 mutations in 30 alleles), loss of splicing site (ten mutations in 20 alleles), missense (four mutations in six alleles), in-frame deletion (two mutations in two alleles), gross deletion encompassing exon 1 to exon 5 (one mutation in two alleles), and loss of initiation (one mutation in one allele; Table 2). Most of these mutant alleles (93.3%, 112/120) would result in a truncated protein if expressed (Appendix 3), and most of the transcripts would be degraded by nonsense-mediated decay. These mutations were spread into all 12 coding exons, with enrichment in exons 5 and 11 (Figure 4). Four mutations, c.253C>T (p.R85*), c.1183C>T

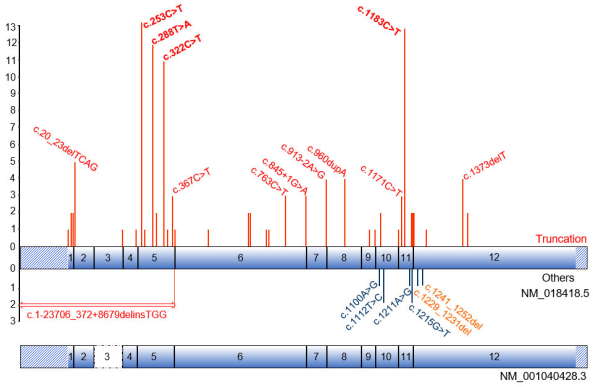

Figure 4. A schematic diagram of the mutation spectrum frequency in *SPATA7*. The two horizontal bars represent the coding regions based on two alternative splicing isoforms. Most loss-of-function mutations are listed on the top of the upper bar. A gross deletion involving the first five exons, four missense mutations, and two in-frame deletions are listed under the upper bar. The line height indicates the number of mutated alleles in 60 families.

(p.R395*), c.288T>A (p.C96*), and c.322C>T (p.R108*), were relatively common and affected 13, 13, 12, and 11 of the 120 mutant alleles, respectively (Table 2 and Figure 4). All of these mutations are rare in the general population based on existing databases (Table 2).

Of the 78 patients from 60 families with biallelic mutations in *SPATA7*, the clinical diagnosis was LCA in 41 families (52 patients), RP in ten families (11 patients), juvenile RP in six families (eight patients), CORD in three families (five patients), and myopia in one family (two patients; Appendix 2) [1-33]. Among siblings in one family with a homozygous c.1112T>C (p.I371T) mutation, a 52-year-old brother had RP, and his 48-year-old sister had CORD [24]. A male patient who had been diagnosed with CORD at 9 years old was subsequently diagnosed with RP at 21 years of age [18]. Clinical information on the other three patients diagnosed with CORD was not available. Eight patients diagnosed with juvenile RP had symptoms in the first few years after birth, but six of them were examined they were 7 years old (Appendix 2). Among the 11 patients diagnosed with RP, there were no clinical data available for six patients from six families. For the other five patients with RP, all underwent examination at the age of 25 years old or older: Two had symptoms at the age of 22 or 25 years, one had no symptoms at the age of 26 years, and the symptoms of the other two patients were not documented. Overall, in 28 of the 60 families, the initial symptom recorded was poor vision or nystagmus or both in 24 probands and night blindness in four probands. Age at onset varied from 3 months to no symptoms at age 26 years [5]. Visual acuity was recorded in 33 of 78 patients, and it ranged from no light perception to nearly normal. Four affected children had no light perception, and five patients had best visual acuity better than 0.5 (20/20; Appendix 2).

Fundus color images were available for 15 patients, including six patients in this cohort and ten patients in published literature [1,3,7,12,24,30]. A documentary record of the fundus changes was available for four cases in this cohort and 19 cases in published literature [1-3,5,7,12,14,18,26]. Based on these records, the fundus may appear normal or nearly normal at an early stage (i.e., a few months after birth), with mild narrow arterioles and a relatively well-preserved macular region, with possible mild hypopigmentation in the midperipheral region. However, within a few years, retinal degeneration gradually progresses to widespread atrophy of the RPE, leading to diffuse hypopigmented grayish-white spots or mottled degeneration in the midperipheral region. Minimal intraretinal pigmentation may appear by school age, with a gradual change to salt-and-pepper appearance. Bone spicule-like pigmentation was not observed in patients until at least the age of 25 years but was common in patients aged approximately 40–50 years old. Narrow arterioles, a relatively well-preserved macular region, and widespread RPE atrophy resulting in diffuse mottling hypopigmentation in the midperipheral retinal region may be considered early and common fundus changes specific to *SPATA7*-associated retinopathy (Figure 2).

Except age-dependent variations in the disease phenotypes, retinal degeneration and accompanied visual function varied markedly among the individuals with mutations in *SPATA7*, from no symptoms at the age of 26 years old [5] or nearly normal visual acuity [1,3] to early blindness. Significant phenotypic variation was also present in siblings with the same mutations [5,24]. Previous research suggested that a truncation mutation in the C-terminal portion might be associated with milder phenotypes, such as RP [1]. However, several patients with RP did have truncation mutations in the N-terminal region [5,12,15,17]. In addition, two siblings

(F10-II:1 and F10-II:2) with a truncation mutation in the N-terminal region showed myopia without obvious fundus changes. It might be that a truncated protein with partial function is produced by a new start codon downstream of the mutational position, or myopia is an earlier feature than significant fundus changes, which would be similar to a case with mutations in *RBP3* as described in a previous study [37]. As 93.3% of mutations in *SPATA7* are truncation mutations, the location of the truncation mutation does not appear to correlate with the severity of the manifestations in individuals with mutations in *SPATA7*, and there is no firm evidence for other genotype–phenotype correlations. Thus, by exclusion, this suggests that other unknown factors may act as modifiers to affect the severity of the disease phenotype [3,5]. The latter has been well demonstrated in recent studies on other diseases [38]. Sparing of the inferior portion of the retina close to the optic fissure (Figure 2C–F) also suggests that potential intrinsic factors might modify the expression of the diseases. Understanding the role of such factors in ocular diseases and the underlying mechanisms may have therapeutic potential.

In addition, four missense mutations and two in-frame deletions were detected in nine patients from seven families in previous reports [3,13,19,24-26,30]. Except c.1112T>C (p.I371T), all others were compound heterozygous mutations with another truncation mutation. Two members of one family with a homozygous c.1112T>C mutation had different types of HRD: RP in the brother and CORD in the sister [24]. Among the other seven patients, six patients had LCA, and one had RP. The phenotypes of patients with a missense or in-frame deletion appear to be comparable to those of patients with biallelic truncation mutations. The pathogenicity of missense or in-frame deletions requires additional studies because of two unusual facts: 1) If loss-of-function mutations are the main cause of the disease, the phenotypes associated with missense mutations would be expected to be mild; 2) if both missense and loss-of-function mutations are causative, there should be more missense mutations detected, especially in this era of next-generation sequencing.

In summary, mutations in *SPATA7* were identified in ten families with phenotypes varying from LCA (most common) to arRP (less common) to rare early-onset myopia. Two novel truncation mutations were identified, including c.367C>T (p.Q123*) and c.1083–2A>G. The clinical and genetic data in our series, together with a systematic analysis of previously published data, showed that 93.3% (112/120) of mutant alleles in these families were truncation mutations. Narrow arterioles, a relatively well-preserved macular region, and widespread RPE atrophy resulting in diffuse mottling hypopigmentation in the midperipheral retina may be considered early and common fundus changes suggestive of *SPATA7*-associated retinopathy. A genotype–phenotype analysis revealed the characteristics of pathogenic mutations and the potential problem of missense variants, as well as findings suggestive of potential modifiers. The findings of the present study can provide a valuable reference for clinical gene tests as well as for future studies.

APPENDIX 1.

To access the data, click or select the words "Appendix 1." Chromatography of nucleotide sequence variations determined by Sanger sequencing. Pedigrees and individual numbers are shown on the left side, and the corresponding sequence variations are presented on the right side.

APPENDIX 2.

To access the data, click or select the words "Appendix 2." Mutations and associated clinical data of all patients described in this study as well as previously reported studies in literatures

APPENDIX 3.

To access the data, click or select the words "Appendix 3." The proportion of mutant alleles (left), as well as genotypes of *SPATA7* in 60 families (right).

ACKNOWLEDGMENTS

The authors are grateful to the families for their participation. This work was supported by National Natural Science Foundation of China (81371058, 81770965), the Key Projects of Guangzhou (201607020013), and the Fundamental Research Funds of the State Key Laboratory of Ophthalmology. Qingjiong Zhang is a recipient of National Science Fund for Distinguished Young Scholars.

REFERENCES

1. Wang H, den Hollander AI, Moayedi Y, Abulimiti A, Li Y, Collin RW, Hoyng CB, Lopez I, Abboud EB, Al-Rajhi AA, Bray M, Lewis RA, Lupski JR, Mardon G, Koenekoop RK, Chen R. Mutations in SPATA7 cause Leber congenital amaurosis and juvenile retinitis pigmentosa. Am J Hum Genet 2009; 84:380-7. [PMID: 19268277].

2. Perrault I, Hanein S, Gerard X, Delphin N, Fares-Taie L, Gerber S, Pelletier V, Merce E, Dollfus H, Puech B, Defoort-Dhellemmes S, Petersen MD, Zafeiriou D, Munnich A, Kaplan J, Roche O, Rozet JM. Spectrum of SPATA7 mutations in Leber congenital amaurosis and delineation of the associated phenotype. Hum Mutat 2010; 31:E1241-50. [PMID: 20104588].

3. Mackay DS, Ocaka LA, Borman AD, Sergouniotis PI, Henderson RH, Moradi P, Robson AG, Thompson DA, Webster AR, Moore AT. Screening of SPATA7 in patients with Leber congenital amaurosis and severe childhood-onset retinal dystrophy reveals disease-causing mutations. Invest Ophthalmol Vis Sci 2011; 52:3032-8. [PMID: 21310915].

4. Li L, Xiao X, Li S, Jia X, Wang P, Guo X, Jiao X, Zhang Q, Hejtmancik JF. Detection of variants in 15 genes in 87 unrelated Chinese patients with Leber congenital amaurosis. PLoS One 2011; 6:e19458-[PMID: 21602930].

5. Avila-Fernandez A, Corton M, Lopez-Molina MI, Martin-Garrido E, Cantalapiedra D, Fernandez-Sanchez R, Blanco-Kelly F, Riveiro-Alvarez R, Tatu SD, Trujillo-Tiebas MJ, Garcia-Sandoval B, Ayuso C, Cremers FP. Late onset retinitis pigmentosa. Ophthalmology 2011; 118:2523-4. [PMID: 22136677].

6. Neveling K, Collin RW, Gilissen C, van Huet RA, Visser L, Kwint MP, Gijsen SJ, Zonneveld MN, Wieskamp N, de Ligt J, Siemiatkowska AM, Hoefsloot LH, Buckley MF, Kellner U, Branham KE, den Hollander AI, Hoischen A, Hoyng C, Klevering BJ, van den Born LI, Veltman JA, Cremers FP, Scheffer H. Next-generation genetic testing for retinitis pigmentosa. Hum Mutat 2012; 33:963-72. [PMID: 22334370].

7. Kannabiran C, Palavalli L, Jalali S. Mutation of SPATA7 in a family with autosomal recessive early-onset retinitis pigmentosa. J Mol Genet Med 2012; 6:301-3. [PMID: 23300508].

8. Wang X, Wang H, Sun V, Tuan HF, Keser V, Wang K, Ren H, Lopez I, Zaneveld JE, Siddiqui S, Bowles S, Khan A, Salvo J, Jacobson SG, Iannaccone A, Wang F, Birch D, Heckenlively JR, Fishman GA, Traboulsi EI, Li Y, Wheaton D, Koenekoop RK, Chen R. Comprehensive molecular diagnosis of 179 Leber congenital amaurosis and juvenile retinitis pigmentosa patients by targeted next generation sequencing. J Med Genet 2013; 50:674-88. [PMID: 23847139].

9. Xu Y, Guan L, Shen T, Zhang J, Xiao X, Jiang H, Li S, Yang J, Jia X, Yin Y, Guo X, Wang J, Zhang Q. Mutations of 60 known causative genes in 157 families with retinitis pigmentosa based on exome sequencing. Hum Genet 2014; 133:1255-71. [PMID: 24938718].

10. Watson CM, El-Asrag M, Parry DA, Morgan JE, Logan CV, Carr IM, Sheridan E, Charlton R, Johnson CA, Taylor G, Toomes C, McKibbin M, Inglehearn CF, Ali M. Mutation screening of retinal dystrophy patients by targeted capture from tagged pooled DNAs and next generation sequencing. PLoS One 2014; 9:e104281-[PMID: 25133751].

11. Consugar MB, Navarro-Gomez D, Place EM, Bujakowska KM, Sousa ME, Fonseca-Kelly ZD, Taub DG, Janessian M, Wang DY, Au ED, Sims KB, Sweetser DA, Fulton AB, Liu Q, Wiggs JL, Gai X, Pierce EA. Panel-based genetic diagnostic testing for inherited eye diseases is highly accurate and reproducible, and more sensitive for variant detection, than exome sequencing. Genet Med 2015; 17:253-61. [PMID: 25412400].

12. Mayer AK, Mahajnah M, Zobor D, Bonin M, Sharkia R, Wissinger B. Novel homozygous large deletion including the 5′ part of the SPATA7 gene in a consanguineous Israeli Muslim Arab family. Mol Vis 2015; 21:306-15. [PMID: 25814828].

13. Wang H, Wang X, Zou X, Xu S, Li H, Soens ZT, Wang K, Li Y, Dong F, Chen R, Sui R. Comprehensive Molecular Diagnosis of a Large Chinese Leber Congenital Amaurosis Cohort. Invest Ophthalmol Vis Sci 2015; 56:3642-55. [PMID: 26047050].

14. Srilekha S, Arokiasamy T, Srikrupa NN, Umashankar V, Meenakshi S, Sen P, Kapur S, Soumittra N. Homozygosity Mapping in Leber Congenital Amaurosis and Autosomal Recessive Retinitis Pigmentosa in South Indian Families. PLoS One 2015; 10:e0131679-[PMID: 26147992].

15. Sharon D, Banin E. Nonsyndromic retinitis pigmentosa is highly prevalent in the Jerusalem region with a high frequency of founder mutations. Mol Vis 2015; 21:783-92. [PMID: 26261414].

16. Beryozkin A, Shevah E, Kimchi A, Mizrahi-Meissonnier L, Khateb S, Ratnapriya R, Lazar CH, Blumenfeld A, Ben-Yosef T, Hemo Y, Pe'er J, Averbuch E, Sagi M, Boleda A, Gieser L, Zlotogorski A, Falik-Zaccai T, Alimi-Kasem O, Jacobson SG, Chowers I, Swaroop A, Banin E, Sharon D. Whole Exome Sequencing Reveals Mutations in Known Retinal Disease Genes in 33 out of 68 Israeli Families with Inherited Retinopathies. Sci Rep 2015; 5:13187-[PMID: 26306921].

17. Patel N, Aldahmesh MA, Alkuraya H, Anazi S, Alsharif H, Khan AO, Sunker A, Al-Mohsen S, Abboud EB, Nowilaty SR, Alowain M, Al-Zaidan H, Al-Saud B, Alasmari A, Abdel-Salam GM, Abouelhoda M, Abdulwahab FM, Ibrahim N, Naim E, Al-Younes B. A EA, AlIssa A, Hashem M, Buzovetsky O, Xiong Y, Monies D, Altassan N, Shaheen R, Al-Hazzaa SA, Alkuraya FS. Expanding the clinical, allelic, and locus heterogeneity of retinal dystrophies. Genet Med 2016; 18:554-62. [PMID: 26355662].

18. Matsui R, McGuigan Iii DB, Gruzensky ML, Aleman TS, Schwartz SB, Sumaroka A, Koenekoop RK, Cideciyan AV, Jacobson SG. SPATA7: Evolving phenotype from cone-rod dystrophy to retinitis pigmentosa. Ophthalmic Genet 2016; 37:333-8. [PMID: 26854980].

19. Ellingford JM, Barton S, Bhaskar S, O'Sullivan J, Williams SG, Lamb JA, Panda B, Sergouniotis PI, Gillespie RL, Daiger SP, Hall G, Gale T, Lloyd IC, Bishop PN, Ramsden SC, Black GCM. Molecular findings from 537 individuals with inherited retinal disease. J Med Genet 2016; 53:761-7. [PMID: 27208204].

20. Xu Y, Xiao X, Li S, Jia X, Xin W, Wang P, Sun W, Huang L, Guo X, Zhang Q. Molecular genetics of Leber congenital amaurosis in Chinese: New data from 66 probands and mutation overview of 159 probands. Exp Eye Res 2016; 149:93-9. [PMID: 27375279].

21. Alabdullatif MA, Al Dhaibani MA, Khassawneh MY, El-Hattab AW. Chromosomal microarray in a highly consanguineous population: diagnostic yield, utility of regions of homozygosity, and novel mutations. Clin Genet 2017; 91:616-22. [PMID: 27717089].

22. Trujillano D, Bertoli-Avella AM, Kumar Kandaswamy K, Weiss ME, Koster J, Marais A, Paknia O, Schroder R, Garcia-Aznar JM, Werber M, Brandau O, Calvo Del Castillo M, Baldi C, Wessel K, Kishore S, Nahavandi N, Eyaid W, Al Rifai MT, Al-Rumayyan A, Al-Twaijri W, Alothaim A, Alhashem A, Al-Sannaa N, Al-Balwi M, Alfadhel M, Rolfs A, Abou Jamra R. Clinical exome sequencing: results from 2819 samples reflecting 1000 families. Eur J Hum Genet 2017; 25:176-82. [PMID: 27848944].

23. Haer-Wigman L, van Zelst-Stams WA, Pfundt R, van den Born LI, Klaver CC, Verheij JB, Hoyng CB, Breuning MH, Boon CJ, Kievit AJ, Verhoeven VJ, Pott JW, Sallevelt SC, van Hagen JM, Plomp AS, Kroes HY, Lelieveld SH, Hehir-Kwa JY, Castelein S, Nelen M, Scheffer H, Lugtenberg D, Cremers FP, Hoefsloot L, Yntema HG. Diagnostic exome sequencing in 266 Dutch patients with visual impairment. Eur J Hum Genet 2017; 25:591-9. [PMID: 28224992].

24. Feldhaus B, Kohl S, Hortnagel K, Weisschuh N, Zobor D. Novel homozygous mutation in the SPATA7 gene causes autosomal recessive retinal degeneration in a consanguineous German family. Ophthalmic Genet 2018; 39:131-4. [PMID: 28481129].

25. Soens ZT, Branch J, Wu S, Yuan Z, Li Y, Li H, Wang K, Xu M, Rajan L, Motta FL, Simoes RT, Lopez-Solache I, Ajlan R, Birch DG, Zhao P, Porto FB, Sallum J, Koenekoop RK, Sui R, Chen R. Leveraging splice-affecting variant predictors and a minigene validation system to identify Mendelian disease-causing variants among exon-captured variants of uncertain significance. Hum Mutat 2017; 38:1521-33. [PMID: 28714225].

26. Di Iorio V, Karali M, Brunetti-Pierri R, Filippelli M, Di Fruscio G, Pizzo M, Mutarelli M, Nigro V, Testa F, Banfi S, Simonelli F. Clinical and Genetic Evaluation of a Cohort of Pediatric Patients with Severe Inherited Retinal Dystrophies. Genes (Basel) 2017; 8:[PMID: 29053603].

27. Srikrupa NN, Srilekha S, Sen P, Arokiasamy T, Meenakshi S, Bhende M, Kapur S, Soumittra N. Genetic profile and mutation spectrum of Leber congenital amaurosis in a larger Indian cohort using high throughput targeted re-sequencing. Clin Genet 2018; 93:329-39. [PMID: 29068479].

28. Thompson JA, De Roach JN, McLaren TL, Montgomery HE, Hoffmann LH, Campbell IR, Chen FK, Mackey DA, Lamey TM. The genetic profile of Leber congenital amaurosis in an Australian cohort. Mol Genet Genomic Med 2017; 5:652-67. [PMID: 29178642].

29. Porto FBO, Jones EM, Branch J, Soens ZT, Maia IM, Sena IFG, Sampaio SAM, Simoes RT, Chen R. Molecular Screening of 43 Brazilian Families Diagnosed with Leber Congenital Amaurosis or Early-Onset Severe Retinal Dystrophy. Genes (Basel) 2017; 8:[PMID: 29186038].

30. Sengillo JD, Lee W, Bilancia CG, Jobanputra V, Tsang SH. Phenotypic expansion and progression of SPATA7-associated retinitis pigmentosa. Doc Ophthalmol 2018; 136:125-33. [PMID: 29411205].

31. Huang H, Chen Y, Chen H, Ma Y, Chiang PW, Zhong J, Liu X. Asan, Wu J, Su Y, Li X, Deng J, Huang Y, Zhang X, Li Y, Fan N, Wang Y, Tang L, Shen J, Chen M, Zhang X, Te D, Banerjee S, Liu H, Qi M, Yi X. Systematic evaluation of a targeted gene capture sequencing panel for molecular diagnosis of retinitis pigmentosa. PLoS One 2018; 13:e0185237-[PMID: 29641573].

32. Wang L, Zhang J, Chen N, Wang L, Zhang F, Ma Z, Li G, Yang L. Application of Whole Exome and Targeted Panel Sequencing in the Clinical Molecular Diagnosis of 319 Chinese Families with Inherited Retinal Dystrophy and Comparison Study. Genes (Basel) 2018; 9:[PMID: 30029497].

33. Patel N, Alkuraya H, Alzahrani SS, Nowailaty SR, Seidahmed MZ, Alhemidan A, Ben-Omran T, Ghazi NG, Al-Aqeel A, Al-Owain M, Alzaidan HI, Faqeih E, Kurdi W, Rahbeeni Z, Ibrahim N, Abdulwahab F, Hashem M, Shaheen R, Abouelhoda M, Monies D, Khan AO, Aldahmesh MA, Alkuraya FS. Mutations in known disease genes account for the majority of autosomal recessive retinal dystrophies. Clin Genet 2018; 94:554-63. [PMID: 30054919].

34. Sun W, Xiao X, Li S, Jia X, Wang P, Zhang Q. Germline Mutations in CTNNB1 Associated With Syndromic FEVR or Norrie Disease. Invest Ophthalmol Vis Sci 2019; 60:93-7. [PMID: 30640974].

35. Wang P, Li S, Sun W, Xiao X, Jia X, Liu M, Xu L, Long Y, Zhang Q. An Ophthalmic Targeted Exome Sequencing Panel as a Powerful Tool to Identify Causative Mutations in Patients Suspected of Hereditary Eye Diseases. Transl Vis Sci Technol 2019; 8:21-[PMID: 31106028].

36. Zhou L, Xiao X, Li S, Jia X, Wang P, Sun W, Zhang F, Li J, Li T, Zhang Q. Phenotypic characterization of patients with early-onset high myopia due to mutations in COL2A1 or COL11A1: Why not Stickler syndrome? Mol Vis 2018; 24:560-73. [PMID: 30181686].

37. Arno G, Hull S, Robson AG, Holder GE, Cheetham ME, Webster AR, Plagnol V, Moore AT. Lack of Interphotoreceptor Retinoid Binding Protein Caused by Homozygous Mutation of RBP3 Is Associated With High Myopia and Retinal Dystrophy. Invest Ophthalmol Vis Sci 2015; 56:2358-65. [PMID: 25766589].

38. Gifford CA, Ranade SS, Samarakoon R, Salunga HT, de Soysa TY, Huang Y, Zhou P, Elfenbein A, Wyman SK, Bui YK, Cordes Metzler KR, Ursell P, Ivey KN, Srivastava D. Oligogenic inheritance of a human heart disease involving a genetic modifier. Science 2019; 364:865-70. [PMID: 31147515].

Articles are provided courtesy of Emory University and the Zhongshan Ophthalmic Center, Sun Yat-sen University, P.R. China. The print version of this article was created on 2 December 2019. This reflects all typographical corrections and errata to the article through that date. Details of any changes may be found in the online version of the article.